A Network-cognizant Aggregate-frequency Reduced-order Power System Dynamical Model

Bo Chen, Abdullah Al-Digs, and Yu Christine Chen
Department of Electrical and Computer Engineering
The University of British Columbia
Vancouver, BC V6T 1Z4
Email: {cbhp1993, aldigs, chen}@ece.ubc.ca

***Abstract*—This paper presents a reduced second-order power-system dynamical model that accounts for locational effects of load disturbances on system frequency dynamics over time scales corresponding to inertial and primary-frequency response. The locational aspects are retained in the proposed model by incorporating linearized power-flow balance into differential equations that describe synchronous-generator dynamics. Individual synchronous-generator speed dynamics are then combined into a single aggregate frequency state via weighting factors that can be tuned to maximize the accuracy of the reduced-order model. The proposed reduced-order model is general in the sense that its parameters are related to those of the original full-order model in analytical closed form, so that it can be constructed easily for different systems. Time-domain simulations demonstrate the accuracy of the reduced-order model with various choices of weighting factors and highlight the effect of load disturbance location on aggregate-frequency dynamics.**

I. Introduction

Model-order reduction has been studied extensively for a wide range of applications in the context of power system static and dynamic simulation, analysis, and control (see, e.g., [1] and references therein). The power system is a complex critical infrastructure that is geographically expansive. So reduced-order models are prudent and often necessary to capture only the most relevant features for a particular problem setting due to limitations in analytical tools or computing resources. For example, reduced-order models have been developed to study the power-flow problem [2], transient stability [3], and interarea oscillations [4], to name a few. In this paper, we develop a reduced-order aggregate-frequency dynamical model that focuses on time scales corresponding to system inertial and primary-frequency response. Such a model is potentially useful to tackle a multitude of contemporary power-system problems, such as conducting dynamic contingency analysis, assessing frequency deviations due to renewable resource variations, and optimizing placement and sizing of distributed energy resources to provide frequency regulation support.

Since we aim to capture inertial and primary-frequency response in a reduced-order model, our approach begins by adopting a third-order model for each synchronous generator, capturing its rotor-angle position, rotor-angle speed, and governor dynamics. We further formulate linearized power-flow equations and incorporate them into the generator dynamical equations, thereby reducing the standard power-system differential-algebraic-equation model into one that contains only differential equations. In this way, the network topology is embedded within the original full-order system dynamical model, and the locational effects of different load disturbances on frequency response are captured. Next, by applying tuneable weighting factors to each synchronous-generator speed state, we obtain a single aggregate frequency that represents a weighted average of all generator speeds. Here, the weighting factors may be designed to, e.g., minimize the error between the reduced- and the full-order models.

Most related prior work in power system dynamic model-order reduction can be broadly categorized into algorithmic or numerical approaches. Algorithmic methods, such as repeated time-domain simulations [3], singular perturbation techniques [4], and weak-coupling identification [5], have been used to identify coherent groups of generators within a large-scale power system. These and application of numerical techniques, such as modal truncation [6], selective modal analysis [7], and Krylov-subspace methods [8] are generally deployed on a detailed higher-order dynamical model. Typically, due to the algorithmic and numerical nature of these methods, they are unable to relate the parameters of the original full-order system to those of the reduced-order one once it is constructed. Recent work has addressed this issue by analytically reducing the full-order model while retaining original-system parameters [9]–[11]. Our approach in this paper begins with similar setup as in [10], [11], and the resulting reduced-order model also retains parameters of the original model in closed form. However, our proposed method differs in the following two aspects. First, by choosing the contribution of each generator speed to the aggregate-frequency response, we have the flexibility of tuning the reduced-order model so that its dynamical response more closely matches that of the original full-order system. Furthermore, by embedding the power-flow constraints within the reduced-order model, it can distinguish between dynamics arising from load disturbances that occur at different locations in the network.

II. System Description

Consider a power transmission network with N buses collected in the set $\mathcal{N} = \{1, \ldots, N\}$ and transmission lines in the set $\mathcal{E} \subset \mathcal{N} \times \mathcal{N}$. Let $V_k(t) = |V_k(t)|\angle\theta_k(t)$ represent the voltage phasor at bus k and time t. Denote,

by $\mathcal{G} = \{1, \ldots, G\} \subset \mathcal{N}$, the set of G buses that are connected to conventional turbine-based generators. Further denote, by $\mathcal{L} = \mathcal{N} \setminus \mathcal{G} = \{G+1, \ldots, N\}$, the set of L load buses, which are connected to only non-frequency-sensitive loads, e.g., constant-power loads. A transmission line with current flowing from bus k to ℓ is denoted by $(k, \ell) \in \mathcal{E}$.

A. Power-flow Model

Transmission line (k, ℓ) is modelled using the lumped-element Π-model with series admittance $y_{k\ell} = y_{\ell k} = g_{k\ell} + \mathrm{j}b_{k\ell} \in \mathbb{C} \setminus \{0\}$ and shunt admittance $y^{\mathrm{sh}}_{k\ell} = g^{\mathrm{sh}}_{k\ell} + \mathrm{j}b^{\mathrm{sh}}_{k\ell} \in \mathbb{C} \setminus \{0\}$ on both ends of the line. The active-power balance at bus $k \in \mathcal{N}$ is given by

$$0 = P_k(t) - \sum_{\ell \in \mathcal{N}_k} P_{k\ell}(t), \tag{1}$$

where $P_k(t)$ is the net active-power injection at bus k, $\mathcal{N}_k$ is the set of buses electrically connected to bus k, and $P_{k\ell}(t)$ represents the active-power flow in line (k, ℓ).

1) AC Power-flow Formulation: If bus k is a load bus, i.e., $k \in \mathcal{L}$, then

$$P_k(t) = P_{\mathrm{L},k}(t), \tag{2}$$

where $P_{\mathrm{L},k}(t)$ is the non-frequency-sensitive active-power injection at bus k, which is a negative quantity if it corresponds to a constant-power load. On the other hand, if bus k is connected to a synchronous generator, i.e., $k \in \mathcal{G}$, then

$$P_k(t) = P_{\mathrm{L},k}(t) + P^{\mathrm{e}}_k(t), \tag{3}$$

where, similar to (2), $P_{\mathrm{L},k}(t)$ is the non-frequency-sensitive active-power injection at bus k. As for $P^{\mathrm{e}}_k(t)$ in (3), using the classical synchronous-machine model for generator $k \in \mathcal{G}$, which comprises a constant voltage E_k behind the transient reactance $\mathrm{j}X'_{d,k}$, $P^{\mathrm{e}}_k(t)$ can be expressed as [12]

$$P^{\mathrm{e}}_k(t) = \frac{E_k |V_k(t)|}{X'_{d,k}} \sin(\delta_k(t) - \theta_k(t)), \tag{4}$$

where $\delta_k(t)$ denotes the rotor electrical angular position of generator k. Finally, following standard power-flow computations, $P_{k\ell}(t)$ in (1) is given by

$$\begin{aligned} P_{k\ell}(t) = {} & |V_k(t)|^2 (g^{\mathrm{sh}}_{k\ell} + g_{k\ell}) \\ & - |V_k(t)||V_\ell(t)| g_{k\ell} \cos(\theta_k(t) - \theta_\ell(t)) \\ & - |V_k(t)||V_\ell(t)| b_{k\ell} \sin(\theta_k(t) - \theta_\ell(t)). \end{aligned} \tag{5}$$

2) DC Power-flow Approximations: In transmission networks, the line resistance is much smaller than its reactance, i.e., for line (k, ℓ), $g_{k\ell} << b_{k\ell}$ and $g^{\mathrm{sh}}_{k\ell} << b^{\mathrm{sh}}_{k\ell}$, so we can approximate $y_{k\ell} = y_{\ell k} \approx \mathrm{j}b_{k\ell}$ and $y^{\mathrm{sh}}_{k\ell} \approx \mathrm{j}b^{\mathrm{sh}}_{k\ell}$. Also, under typical operating conditions, the voltage phase-angle differences between two buses are small, i.e., $\theta_{k\ell} << 1$, for all $k, \ell \in \mathcal{N}$, and $\delta_g - \theta_g << 1$ for all $g \in \mathcal{G}$. Under these assumptions, it follows that $\sin(\theta_k - \theta_\ell) \approx \theta_k - \theta_\ell$ and $\sin(\delta_k - \theta_k) \approx \delta_k - \theta_k$. Finally, in the per-unit system, the numerical values of voltage magnitudes are typically near 1 p.u., i.e., $|V_k| \approx 1$, for all $k \in \mathcal{N}$, and $E_g \approx 1$, for all $g \in \mathcal{G}$. Taken together, these so-called DC assumptions help to simplify (5) as

$$P_{k\ell}(t) = -b_{k\ell}(\theta_k(t) - \theta_\ell(t)). \tag{6}$$

Similarly, (4) simplifies as

$$P^{\mathrm{e}}_k(t) = \frac{1}{X'_{d,k}} (\delta_k(t) - \theta_k(t)). \tag{7}$$

B. Synchronous-generator Dynamical Model

Dynamics of synchronous generator $g \in \mathcal{G}$ can be modelled as follows. For each generator $g \in \mathcal{G}$, let $\delta_g(t)$ and $\omega_g(t)$ denote its rotor electrical angular position and speed, respectively. Further let $P^{\mathrm{m}}_g(t)$ denote its turbine mechanical power. Assume each generator initially operates at the steady-state equilibrium point with $\omega_g(0) = \omega_{\mathrm{s}} = 2\pi 60\,\mathrm{rad/s}$, the synchronous frequency. Defining $\Delta\omega_g := \omega_g - \omega_{\mathrm{s}}$, dynamics of generator $g \in \mathcal{G}$ can be described by the following third-order system:

$$\begin{aligned} \dot{\delta}_g(t) &= \Delta\omega_g(t), \\ M_g \Delta\dot{\omega}_g(t) &= P^{\mathrm{m}}_g(t) - D_g \Delta\omega_g(t) - \sum_{\ell \in \mathcal{N}_g} P_{g\ell}(t) + P_{\mathrm{L},g}(t), \\ \tau_g \dot{P}^{\mathrm{m}}_g(t) &= P^{\mathrm{r}}_g - P^{\mathrm{m}}_g(t) - R_g \Delta\omega_g(t), \end{aligned} \tag{8}$$

where M_g and D_g denote, respectively, the inertia and damping constants, and τ_g, P^{r}_g, and R_g denote the governor time constant, reference power input, and *inverse*[1] droop constant, respectively. The system in (8) consists of the classical synchronous-machine model combined with a speed-governor model [12].

In (8), the generator dynamics are coupled to the network through the $\sum_{\ell \in \mathcal{N}_g} P_{g\ell}(t)$, thereby accounting for network effects on machine dynamics. Motivated by this, we aim to develop a corresponding reduced-order aggregate-frequency model for the entire system, which incorporates network effects. Before delving into these aspects below, we first combine synchronous-generator dynamics in (8) with the approximate power-flow equations in (6)–(7).

C. Power-system Dynamical Model

With the individual-bus power balance and single-generator dynamic equations described thus far, we next combine them into a full-order system dynamical model. We begin by defining relevant vector variables as follows. For the set of synchronous generators $\mathcal{G}$, collect rotor angular positions and variation in their speeds into vectors $\delta_{\mathcal{G}} = [\delta_1, \ldots, \delta_G]^{\mathrm{T}}$ and $\Delta\omega_{\mathcal{G}} = [\Delta\omega_1, \ldots, \Delta\omega_G]^{\mathrm{T}}$, respectively. Similarly, collect the voltage angles of generator buses and non-frequency-responsive injections at these buses into $\theta_{\mathcal{G}} = [\theta_1, \ldots, \theta_G]^{\mathrm{T}}$ and $P_{\mathcal{G}} = [P_{\mathrm{L},1}, \ldots, P_{\mathrm{L},G}]^{\mathrm{T}}$, respectively. Analogously, collect these quantities for the set of load buses into $\theta_{\mathcal{L}} = [\theta_{G+1}, \ldots, \theta_N]^{\mathrm{T}}$ and $P_{\mathcal{L}} = [P_{\mathrm{L},G+1}, \ldots, P_{\mathrm{L},N}]^{\mathrm{T}}$.

[1] In most reference textbooks, R_g refers to the droop constant; in this paper, we deviate from the standard to contain notational burden later.

1) Power-flow Algebraic Equations: Using the notation established above, and by substituting (3) and (6) into (1), we can express the active-power balance at generator buses compactly in matrix form as[2]

$$\mathbb{0}_G = P_{\mathcal{G}}(t)+\text{diag}\left(\frac{\mathbb{1}_G}{X'_d}\right)\delta_{\mathcal{G}}(t)-B_{\mathcal{GG}}\theta_{\mathcal{G}}(t)-B_{\mathcal{GL}}\theta_{\mathcal{L}}(t), \quad (9)$$

where $X'_d = [X'_{d,1},\ldots,X'_{d,G}]^{\mathrm{T}}$, and matrices $B_{\mathcal{GG}}$ and $B_{\mathcal{GL}}$ are constructed appropriately using (6) in conjunction with the network topology. Similarly, by substituting (2) and (6) into (1), the active-power balance at load buses can be compactly expressed as

$$\mathbb{0}_L = P_{\mathcal{L}}(t) - B_{\mathcal{LG}}\theta_{\mathcal{G}}(t) - B_{\mathcal{LL}}\theta_{\mathcal{L}}(t), \quad (10)$$

where, again, entries of $B_{\mathcal{LG}}$ and $B_{\mathcal{LL}}$ are evaluated using (6) based on the network topology.

To further reduce notational burden in (9) and (10), define $\theta := [\theta_{\mathcal{G}}^{\mathrm{T}}, \theta_{\mathcal{L}}^{\mathrm{T}}]^{\mathrm{T}}$ and $P := [P_{\mathcal{G}}^{\mathrm{T}}, P_{\mathcal{L}}^{\mathrm{T}}]^{\mathrm{T}}$. Then, we combine (9) and (10) and rearrange the resultant to get

$$\theta(t) = B^{-1}\left(D\delta_{\mathcal{G}}(t) + P(t)\right), \quad (11)$$

where[3]

$$B = \begin{bmatrix} B_{\mathcal{GG}} & B_{\mathcal{GL}} \\ B_{\mathcal{LG}} & B_{\mathcal{LL}} \end{bmatrix}, \quad D = \begin{bmatrix} \text{diag}\left(\frac{\mathbb{1}_G}{X'_d}\right) \\ \mathbb{0}_{L\times G} \end{bmatrix}. \quad (12)$$

Entries in and structures of matrices $B_{\mathcal{GG}}$, $B_{\mathcal{GL}}$, $B_{\mathcal{LG}}$, and $B_{\mathcal{LL}}$ are detailed in Appendix A. Note that by making use of partitioned matrix inversion, and assuming relevant submatrices are invertible, (11) can be simplified as [13]

$$\theta(t) = A\delta_{\mathcal{G}}(t) + B^{-1}P(t), \quad (13)$$

where

$$A = \begin{bmatrix} \text{diag}(\mathbb{1}_G) \\ -B_{\mathcal{LL}}^{-1}B_{\mathcal{LG}} \end{bmatrix}(B_{\mathcal{GG}} - B_{\mathcal{GL}}B_{\mathcal{LL}}^{-1}B_{\mathcal{LG}})^{-1}\text{diag}\left(\frac{\mathbb{1}_G}{X'_d}\right). \quad (14)$$

2) Synchronous-generator Dynamic Equations: For the set of synchronous generators $\mathcal{G}$, collect turbine mechanical power states and reference power inputs into $P_{\mathcal{G}}^{\mathrm{m}} = [P_1^{\mathrm{m}},\ldots,P_G^{\mathrm{m}}]^{\mathrm{T}}$ and $P_{\mathcal{G}}^{\mathrm{r}} = [P_1^{\mathrm{r}},\ldots,P_G^{\mathrm{r}}]^{\mathrm{T}}$, respectively. Then, we can express generator dynamics in (8) compactly in matrix form as

$$\dot{\delta}_{\mathcal{G}}(t) = \Delta\omega_{\mathcal{G}}(t), \quad (15)$$

$$\text{diag}(M_{\mathcal{G}})\Delta\dot{\omega}_{\mathcal{G}}(t) = P_{\mathcal{G}}^{\mathrm{m}}(t) - \text{diag}(D_{\mathcal{G}})\Delta\omega_{\mathcal{G}}(t) + K\theta(t) + P_{\mathcal{G}}(t), \quad (16)$$

$$\text{diag}(\tau_{\mathcal{G}})\dot{P}_{\mathcal{G}}^{\mathrm{m}}(t) = P_{\mathcal{G}}^{\mathrm{r}} - P_{\mathcal{G}}^{\mathrm{m}}(t) - \text{diag}(R_{\mathcal{G}})\Delta\omega_{\mathcal{G}}(t), \quad (17)$$

where $M_{\mathcal{G}} = [M_1,\ldots,M_G]^{\mathrm{T}}$, $D_{\mathcal{G}} = [D_1,\ldots,D_G]^{\mathrm{T}}$, $\tau_{\mathcal{G}} = [\tau_1,\ldots,\tau_G]^{\mathrm{T}}$, and $R_{\mathcal{G}} = [R_1,\ldots,R_G]^{\mathrm{T}}$. Also, in (16), the entries of $K \in \mathbb{R}^{G\times L}$ are formed by appropriately evaluating (6) based on the network topology as

$$K = -\left[\text{diag}\left(\frac{\mathbb{1}_G}{X'_d}\right) + B_{\mathcal{GG}} \quad B_{\mathcal{GL}}\right]. \quad (18)$$

[2]The M-dimensional vectors with all 0s and 1s are denoted by $\mathbb{0}_M$ and $\mathbb{1}_M$, respectively. The diagonal matrix $\text{diag}(x)$ is formed with entries of the vector x stacked on the main diagonal; and $\text{diag}(x/y)$ forms a diagonal matrix with the ith diagonal entry given by x_i/y_i, where x_i and y_i are the ith entries of vectors x and y, respectively.

[3]The M by N matrix of all 0s is denoted by $\mathbb{0}_{M\times N}$.

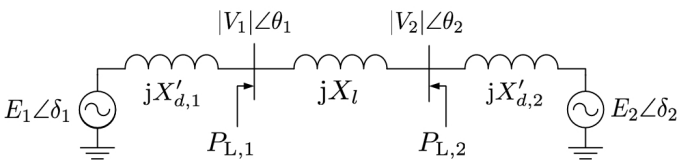

Fig. 1: Network topology for two-bus system.

3) Full-order Power-system Model: By substituting (11) into (16), we obtain the full-order power-system dynamical model as follows:

$$\dot{\delta}_{\mathcal{G}}(t) = \Delta\omega_{\mathcal{G}}(t), \quad (19)$$

$$\Delta\dot{\omega}_{\mathcal{G}}(t) = \text{diag}(M_{\mathcal{G}})^{-1}\big(P_{\mathcal{G}}^{\mathrm{m}}(t) - \text{diag}(D_{\mathcal{G}})\Delta\omega_{\mathcal{G}}(t) + H\delta_{\mathcal{G}}(t) + WP(t)\big), \quad (20)$$

$$\dot{P}_{\mathcal{G}}^{\mathrm{m}}(t) = \text{diag}(\tau_{\mathcal{G}})^{-1}\left(P_{\mathcal{G}}^{\mathrm{r}} - P_{\mathcal{G}}^{\mathrm{m}}(t) - \text{diag}(R_{\mathcal{G}})\Delta\omega_{\mathcal{G}}(t)\right), \quad (21)$$

where matrices $H \in \mathbb{R}^{G\times G}$ and $W \in \mathbb{R}^{G\times N}$ capture network effects and are expressed as, respectively,

$$H = KB^{-1}D = KA, \quad (22)$$

$$W = KB^{-1} + \left[\text{diag}(\mathbb{1}_G) \quad \mathbb{0}_{G\times L}\right]. \quad (23)$$

Furthermore, with a view that entries of $P(t)$ represent inputs to the power system, entries of W indicate the effects of load variations at different buses on the speed dynamics of each machine.

Next, we illustrate the ideas presented above on forming the full-order power-system model via an example.

Example 1 (Two-bus System): In this example, we consider the two-bus test system shown in Fig. 1, where each bus is connected to a synchronous generator as well as non-frequency-dependent injections. Using the notation established in (12), for this system, we have

$$B = \begin{bmatrix} \frac{1}{X'_{d,1}} + \frac{1}{X_l} & -\frac{1}{X_l} \\ -\frac{1}{X_l} & \frac{1}{X'_{d,1}} + \frac{1}{X_l} \end{bmatrix}, \quad D = \begin{bmatrix} \frac{1}{X'_{d,1}} & 0 \\ 0 & \frac{1}{X'_{d,2}} \end{bmatrix}.$$

Furthermore, making use of (18), we get that

$$K = \begin{bmatrix} -\frac{1}{X_l} & \frac{1}{X_l} \\ \frac{1}{X_l} & -\frac{1}{X_l} \end{bmatrix}.$$

Then, using the expressions for B, D, and K above, we can evaluate (22) to obtain

$$H = \frac{1}{X'_{d,1} + X_l + X'_{d,2}}\begin{bmatrix} -1 & 1 \\ 1 & -1 \end{bmatrix},$$

as expected via direct inspection of Fig. 1. Finally, using (23) for the two-bus system, we get that

$$W = \frac{1}{X'_{d,1} + X_l + X'_{d,2}}\begin{bmatrix} X'_{d,2} + X_l & X'_{d,2} \\ X'_{d,1} & X'_{d,1} + X_l \end{bmatrix}.$$

As shown above, under DC assumptions, the input matrix W is expressed as a function of only the network parameters. The entries in W highlight the effect of load variations at different buses on the speed dynamics of each synchronous machine. ■

III. Model-order Reduction

In this section, we sequentially present several reductions of the full-order system in (19)–(21). Our goal is to obtain an aggregate-frequency model that accounts for network effects.

A. Aggregate-frequency Model

Define system aggregate frequency $\Delta\widetilde{\omega} := c^{\mathrm{T}}\Delta\omega_{\mathcal{G}}$, where the gth entry in $c \in \mathbb{R}^G$ represents the contribution of generator g rotor angular speed to the aggregate frequency. From (20), we get that

$$\begin{aligned}\Delta\dot{\widetilde{\omega}}(t) &= c^{\mathrm{T}}\Delta\dot{\omega}_{\mathcal{G}}(t)\\ &= c^{\mathrm{T}}\mathrm{diag}(M_{\mathcal{G}})^{-1}\big(P^{\mathrm{m}}_{\mathcal{G}}(t) - \mathrm{diag}(D_{\mathcal{G}})\Delta\omega_{\mathcal{G}}(t)\\ &\qquad + H\delta_{\mathcal{G}}(t) + WP(t)\big). \end{aligned} \tag{24}$$

Also define scalar variable $\widetilde{\delta} := c^{\mathrm{T}}\mathrm{diag}(M_{\mathcal{G}})^{-1}H\delta_{\mathcal{G}}$, and from (19), we have that

$$\dot{\widetilde{\delta}}(t) = c^{\mathrm{T}}\mathrm{diag}(M_{\mathcal{G}})^{-1}H\Delta\omega_{\mathcal{G}}(t). \tag{25}$$

The governor dynamics for all generators are retained as in (21). Later, in Section III-C, we will develop a reduced governor state for the entire system.

Example 2 (Special Case–Canonical Two-area Reduced-order Model): In order to study interarea oscillations in the canonical two-area power system, it is common practice to establish a two-machine interarea equivalent circuit [1]. This system's structure is similar to the one shown in Fig. 1, except that the loads $P_{\mathrm{L},1} = P_{\mathrm{L},2} = 0$. The swing equations for the two-machine equivalent can then be combined to form a reduced second-order system that is similar in form to the single-machine swing equation [1]. In this example, we show that, with appropriate choice of weighting factor c, we recover this reduced-order system, which is well established in the literature. To do so, choose $c = [1, -1]^{\mathrm{T}}$, so that $\Delta\widetilde{\omega} = \Delta\omega_1 - \Delta\omega_2$. For simplicity, in addition to setting $P_{\mathrm{L},1} = P_{\mathrm{L},2} = 0$, also let damping constants $D_1 = D_2 = 0$. Then, (24) can be expressed as

$$\Delta\dot{\widetilde{\omega}}(t) = M_1^{-1}P_1^{\mathrm{m}}(t) - M_2^{-1}P_2^{\mathrm{m}}(t) + \widetilde{\delta}(t), \tag{26}$$

and, based on (25), as well as H evaluated from Example 1,

$$\dot{\widetilde{\delta}}(t) = -\frac{M_1^{-1} + M_2^{-1}}{X'_{d,1} + X_l + X'_{d,2}}\Delta\widetilde{\omega}(t). \tag{27}$$

Taken together, (27) and (26) form the proposed aggregate-frequency model with $c = [1, -1]^{\mathrm{T}}$.

Next, to show that this model is equivalent to the reduced second-order system model in [1], we define auxiliary angle variable

$$\overline{\delta} := -\left(\frac{M_1^{-1} + M_2^{-1}}{X'_{d,1} + X_l + X'_{d,2}}\right)^{-1}\widetilde{\delta}, \tag{28}$$

so that $\dot{\overline{\delta}} = \Delta\widetilde{\omega}$, (26) can then be expressed as

$$\begin{aligned}\Delta\dot{\widetilde{\omega}}(t) &= M_1^{-1}P_1^{\mathrm{m}}(t) - M_2^{-1}P_2^{\mathrm{m}}(t)\\ &\quad - \frac{M_1^{-1} + M_2^{-1}}{X'_{d,1} + X_l + X'_{d,2}}\overline{\delta}(t).\end{aligned} \tag{29}$$

Furthermore, by defining aggregate quantities

$$\overline{M} := \frac{M_1M_2}{M_1 + M_2}, \quad \overline{P}^{\mathrm{m}} := \frac{M_2P_1^{\mathrm{m}} - M_1P_2^{\mathrm{m}}}{M_1 + M_2}, \tag{30}$$

we simplify (29) as

$$\overline{M}\Delta\dot{\widetilde{\omega}}(t) = \overline{P}^{\mathrm{m}}(t) - \frac{1}{X'_{d,1} + X_l + X'_{d,2}}\overline{\delta}(t), \tag{31}$$

the structure and form of which are reminiscent of the single-machine swing equation, as desired. ■

B. Common-frequency Model

Assume that the electrical distances between geographically different parts of the network are negligible, so that all generator speeds follow the same transient behaviour [14]. As a direct consequence, in (8), $\Delta\omega_g = \Delta\omega$, for all $g \in \mathcal{G}$. Then, the aggregate-frequency dynamics in (24) become

$$\begin{aligned}c^{\mathrm{T}}\mathbb{1}_G\Delta\dot{\omega}(t) &= c^{\mathrm{T}}\mathrm{diag}(M_{\mathcal{G}})^{-1}\big(P^{\mathrm{m}}_{\mathcal{G}}(t) - D_{\mathcal{G}}\Delta\omega(t)\\ &\qquad + H\delta_{\mathcal{G}}(t) + WP(t)\big).\end{aligned} \tag{32}$$

For simplicity, and without loss of generalization, we impose a normalization condition on the weighting factor c, so that $c^{\mathrm{T}}\mathbb{1}_G = 1$. Also define scalar variable $\delta := c^{\mathrm{T}}\mathrm{diag}(M_{\mathcal{G}})^{-1}H\delta_{\mathcal{G}}$. Then we obtain the following reduced $(2+G)$th-order common-frequency model:

$$\dot{\delta}(t) = H_{\mathrm{eff}}\Delta\omega(t), \tag{33}$$

$$\begin{aligned}\Delta\dot{\omega}(t) &= c^{\mathrm{T}}\mathrm{diag}(M_{\mathcal{G}})^{-1}P^{\mathrm{m}}_{\mathcal{G}}(t) - D_{\mathrm{eff}}\Delta\omega(t)\\ &\qquad + \delta(t) + W_{\mathrm{eff}}P(t),\end{aligned} \tag{34}$$

$$\dot{P}^{\mathrm{m}}_{\mathcal{G}}(t) = \mathrm{diag}(\tau_{\mathcal{G}})^{-1}\left(P^{\mathrm{r}}_{\mathcal{G}} - P^{\mathrm{m}}_{\mathcal{G}}(t) - R_{\mathcal{G}}\Delta\omega(t)\right), \tag{35}$$

where $H_{\mathrm{eff}} \in \mathbb{R}$, $D_{\mathrm{eff}} \in \mathbb{R}$, and $W_{\mathrm{eff}} \in \mathbb{R}^{1\times N}$ are expressed as, respectively,

$$H_{\mathrm{eff}} := c^{\mathrm{T}}\mathrm{diag}(M_{\mathcal{G}})^{-1}H\mathbb{1}_G, \tag{36}$$

$$D_{\mathrm{eff}} := c^{\mathrm{T}}\mathrm{diag}(M_{\mathcal{G}})^{-1}D_{\mathcal{G}}, \tag{37}$$

$$W_{\mathrm{eff}} := c^{\mathrm{T}}\mathrm{diag}(M_{\mathcal{G}})^{-1}W. \tag{38}$$

In this reduced-order model, W_{eff} captures the *effective* locational effects of load changes across the network on aggregate-frequency dynamics, and D_{eff} represents the *effective* damping constant. Furthermore, and of particular note, $H_{\mathrm{eff}} = 0$ because $H\mathbb{1}_G = \mathbb{0}_G$; we offer a proof of this in Appendix B. Assuming that the network topology does not vary, $\dot{\delta}(t) \equiv 0$, so $\delta(t) \equiv \delta(0)$, for $t > 0$, and thus we can remove the dynamic state $\delta(t)$ from the system described by (33)–(35).

C. Aggregate-governor Model

To further reduce the model in (34)–(35) to a second-order system, we aggregate the governor states by defining scalar variable $P^{\mathrm{m}} := c^{\mathrm{T}}\mathrm{diag}(M_{\mathcal{G}})^{-1}P^{\mathrm{m}}_{\mathcal{G}}$ and, using (35), we get

$$\begin{aligned}\dot{P}^{\mathrm{m}}(t) &= c^{\mathrm{T}}\mathrm{diag}(M_{\mathcal{G}})^{-1}\dot{P}^{\mathrm{m}}_{\mathcal{G}}(t)\\ &= c^{\mathrm{T}}\mathrm{diag}(M_{\mathcal{G}})^{-1}\mathrm{diag}(\tau_{\mathcal{G}})^{-1}\\ &\qquad \cdot\left(P^{\mathrm{r}}_{\mathcal{G}} - P^{\mathrm{m}}_{\mathcal{G}}(t) - R_{\mathcal{G}}\Delta\omega(t)\right).\end{aligned} \tag{39}$$

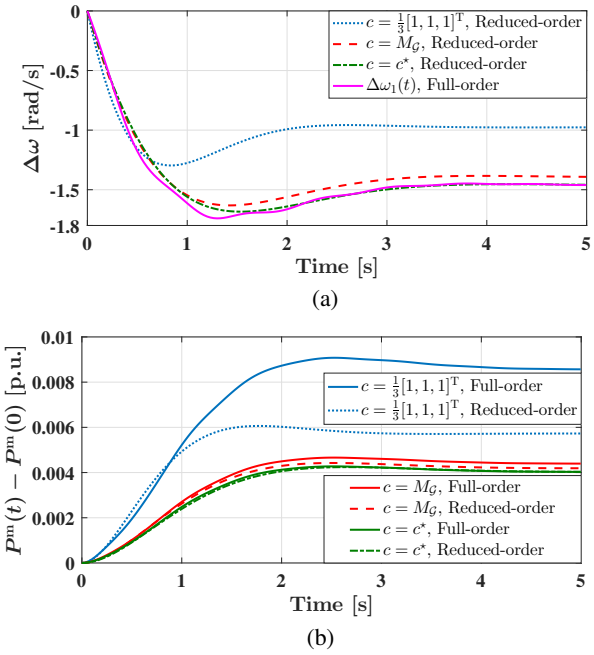

Fig. 2: Comparison of trajectories resulting from full- and reduced-order models with various values of weighting factors c and load disturbance at bus 5, $\Delta P_{\mathrm{L},5} = -0.5\,\mathrm{p.u.}$ (a) Aggregate-frequency deviations. (b) Aggregate-turbine-mechanical-power deviations.

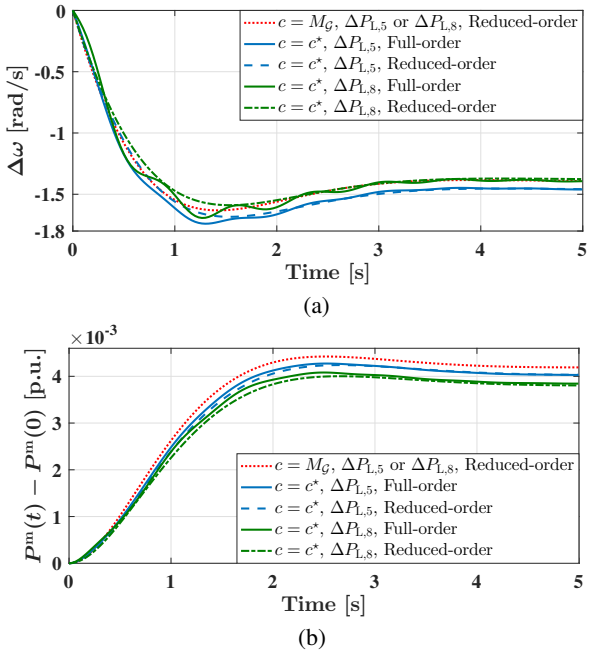

Fig. 3: Comparison of trajectories resulting from full- and reduced-order models with load disturbances at bus 5 or 8, which are distinguishable with $c = c^{\star}$, but not with $c = M_{\mathcal{G}}$. (a) Aggregate-frequency deviations. (b) Aggregate-turbine-mechanical-power deviations.

In practice, the turbine-governor time constants are similar in value, i.e., $\tau_g \approx \tau$, for all $g \in \mathcal{G}$ [15]. Various options have been proposed for the aggregate parameter τ in the literature. The average of all entries in $\tau_{\mathcal{G}}$ is utilized in [9], [16]. More recently, other choices have emerged based on minimizing the error between the reduced- and higher-order models [10]. Assuming that $\tau_g \approx \tau$, for all $g \in \mathcal{G}$, (39) can be simplified, and we arrive at the following reduced second-order model:

$$\begin{aligned} \Delta\dot{\omega}(t) &= P^{\mathrm{m}}(t) - D_{\mathrm{eff}}\Delta\omega(t) + \delta(0) + W_{\mathrm{eff}}P(t), \\ \dot{P}^{\mathrm{m}}(t) &= \tau^{-1}(P^{\mathrm{r}} - P^{\mathrm{m}}(t) - R_{\mathrm{eff}}\Delta\omega(t)), \end{aligned} \tag{40}$$

where the aggregate reference power and *effective* inverse droop constant are, respectively,

$$P^{\mathrm{r}} := c^{\mathrm{T}}\mathrm{diag}(M_{\mathcal{G}})^{-1}P^{\mathrm{r}}_{\mathcal{G}}, \tag{41}$$

$$R_{\mathrm{eff}} := c^{\mathrm{T}}\mathrm{diag}(M_{\mathcal{G}})^{-1}R_{\mathcal{G}}. \tag{42}$$

The reduced-order model in (40) features the following key attributes: (i) it combines all synchronous-generator speeds into one aggregate frequency via the weighting factor c, and (ii) it is network cognizant as it distinguishes the effect of different load changes on system aggregate-frequency dynamics via the vector W_{eff}.

IV. Case Studies

In this section, we demonstrate the flexibility of the proposed reduced-order model and its effectiveness via numerical case studies involving the Western Electricity Coordinating Council (WECC) 3-machine 9-bus test system. The reduced second-order model is verified with time-domain simulations of a nonlinear differential-algebraic model that includes the two-axis synchronous-generator, turbine-governor, and exciter models performed using PSAT [17].

A. Varying Weighting Factor c

Consider the dynamic response following a load increase at bus 5, i.e., $\Delta P_{\mathrm{L},5}(t) := P_{\mathrm{L},5}(t) - P_{\mathrm{L},5}(0) = -0.5\,\mathrm{p.u.}$, $t > 0$. Using various values for the weighting factor c, we compare the mismatch in frequency and mechanical-power dynamics resulting from the full-order model versus the proposed reduced-order one in (40). As shown in Fig. 2 by the blue traces, the naïve choice of $c = \frac{1}{3}[1,1,1]^{\mathrm{T}}$ (i.e., the average) results in large mismatch between the reduced- and full-order models. With $c = M_{\mathcal{G}}$, on the other hand, the mismatch greatly reduces. Finally, as shown by green traces in Fig. 2, the choice $c = c^{\star} = \frac{1}{25}[19,4,2]^{\mathrm{T}}$ (tuned via trial and error) attains nearly perfect match between the dynamic response resulting from the full- and reduced-order models. Note that, in Fig. 2a, comparisons are made against the rotor-angle speed deviations of generator 1, which is representative of the other generators in the full-order model.

B. Varying Location of Load Disturbance

Suppose generators in the WECC system are responding to a generation-load mismatch caused by a load increase located at bus 5 *or* 8, i.e., $\Delta P_{\mathrm{L},5}(t) = -0.5\,\mathrm{p.u.}$ *or* $\Delta P_{\mathrm{L},8}(t) = -0.5$ p.u., $t > 0$. As shown by the solid traces in Fig. 3, the two load disturbances lead to different dynamics in rotor-angle speeds and turbine mechanical powers when the full-order model is used to simulate the system. These locational effects are captured in the reduced-order model with $c = c^{\star}$, as demonstrated by dashed and dash-dot traces that nearly overlap with the solid ones in Fig. 3. In contrast, the effect of disturbance location is not evident with $c = M_g$, because both load disturbances result in the same dynamic response, as shown by the red dotted traces in Fig. 3.

V. Concluding Remarks

In this paper, we present a reduced second-order power system dynamical model, which accounts for locational effects of load disturbances on aggregate-frequency dynamics corresponding to inertial- and primary-frequency response time scales. The utility of the proposed model was demonstrated via numerical case studies involving the WECC test system. Compelling avenues for future work include enhancing the accuracy of the reduced-order model by optimizing the weighting factors, incorporating network losses into the model, and engineering inertial- and primary-frequency response using distributed energy resources.

Appendix

A. Detailing $B_{\mathcal{GG}}$, $B_{\mathcal{GL}}$, $B_{\mathcal{LG}}$, $B_{\mathcal{LL}}$ Matrices

Based on the structures of (9) and (10), matrices $B_{\mathcal{GG}}$, $B_{\mathcal{GL}}$, $B_{\mathcal{LG}}$, and $B_{\mathcal{LL}}$ can be expressed as

$$B_{\mathcal{GG}} = B_{GG} - \operatorname{diag}\left(\begin{bmatrix} B_{GG} & B_{GL}\end{bmatrix} \mathbb{1}_N + \frac{\mathbb{1}_G}{X'_d}\right), \quad (43)$$

$$B_{\mathcal{GL}} = B_{GL}, \quad (44)$$

$$B_{\mathcal{LG}} = B_{LG}, \quad (45)$$

$$B_{\mathcal{LL}} = B_{LL} - \operatorname{diag}\left(\begin{bmatrix} B_{LG} & B_{LL}\end{bmatrix} \mathbb{1}_N\right), \quad (46)$$

where submatrices B_{GG}, B_{GL}, B_{LG}, and B_{LL} are extracted from the standard (and appropriately reordered) network admittance matrix Y for a lossless system, i.e.,

$$Y = \mathrm{j}\begin{bmatrix} B_{GG} & B_{GL} \\ B_{LG} & B_{LL}\end{bmatrix}. \quad (47)$$

B. Showing $H\mathbb{1}_G = \mathbb{0}_G$

Substitute (14) and (18) into (22) to get

$$\begin{aligned} H &= -\left(\operatorname{diag}\left(\frac{\mathbb{1}_G}{X'_d}\right) + J\right) J^{-1}\operatorname{diag}\left(\frac{\mathbb{1}_G}{X'_d}\right) \\ &= -\operatorname{diag}\left(\frac{\mathbb{1}_G}{X'_d}\right)\left(J^{-1}\operatorname{diag}\left(\frac{\mathbb{1}_G}{X'_d}\right) + \operatorname{diag}(\mathbb{1}_G)\right), \end{aligned} \quad (48)$$

where $J = B_{\mathcal{GG}} - B_{\mathcal{GL}}B_{\mathcal{LL}}^{-1}B_{\mathcal{LG}}$. Below, we proceed to show that $H\mathbb{1}_G = \mathbb{0}_G$ by proving that

$$\mathbb{0}_G = \left(J^{-1}\operatorname{diag}\left(\frac{\mathbb{1}_G}{X'_d}\right) + \operatorname{diag}(\mathbb{1}_G)\right)\mathbb{1}_G, \quad (49)$$

which is equivalent to showing that

$$\begin{aligned} \mathbb{0}_G &= \left(\operatorname{diag}\left(\frac{\mathbb{1}_G}{X'_d}\right) + J\right)\mathbb{1}_G \\ &= \frac{\mathbb{1}_G}{X'_d} + B_{\mathcal{GG}}\mathbb{1}_G - B_{\mathcal{GL}}B_{\mathcal{LL}}^{-1}B_{\mathcal{LG}}\mathbb{1}_G. \end{aligned} \quad (50)$$

We proceed to prove (50) as follows. First, using (43), we get

$$\begin{aligned} B_{\mathcal{GG}}\mathbb{1}_G &= B_{GG}\mathbb{1}_G - \operatorname{diag}\left(\begin{bmatrix} B_{GG} & B_{GL}\end{bmatrix}\mathbb{1}_N + \frac{\mathbb{1}_G}{X'_d}\right)\mathbb{1}_G \\ &= B_{GG}\mathbb{1}_G - \begin{bmatrix} B_{GG} & B_{GL}\end{bmatrix}\mathbb{1}_N - \frac{\mathbb{1}_G}{X'_d} \\ &= -B_{GL}\mathbb{1}_L - \frac{\mathbb{1}_G}{X'_d} = -B_{\mathcal{GL}}\mathbb{1}_L - \frac{\mathbb{1}_G}{X'_d}. \end{aligned} \quad (51)$$

where the last equality above follows by substituting (44). Next, using (46), we have that

$$\begin{aligned} B_{\mathcal{LL}}\mathbb{1}_L &= B_{LL}\mathbb{1}_L - \operatorname{diag}\left(\begin{bmatrix} B_{LG} & B_{LL}\end{bmatrix}\mathbb{1}_N\right)\mathbb{1}_G \\ &= B_{LL}\mathbb{1}_L - \begin{bmatrix} B_{LG} & B_{LL}\end{bmatrix}\mathbb{1}_N \\ &= -B_{LG}\mathbb{1}_G = -B_{\mathcal{LG}}\mathbb{1}_G, \end{aligned} \quad (52)$$

where the last equality above follows by substituting (45). Finally, we substitute (51) and (52) into the right-hand side of (50) to obtain

$$\frac{\mathbb{1}_G}{X'_d} - B_{\mathcal{GL}}\mathbb{1}_L - \frac{\mathbb{1}_G}{X'_d} + B_{\mathcal{GL}}B_{\mathcal{LL}}^{-1}B_{\mathcal{LL}}\mathbb{1}_L = \mathbb{0}_G, \quad (53)$$

and $H\mathbb{1}_G = \mathbb{0}_G$, as desired.

References

[1] A. Chakrabortty and J. H. Chow, *Measurement-Based Methods for Model Reduction of Power Systems Using Synchrophasors*. New York, NY: Springer New York, 2013, pp. 159–197.

[2] B. Stott, J. Jardim, and O. Alsac, "DC power flow revisited," *IEEE Transactions on Power Systems*, vol. 24, no. 3, pp. 1290 – 1300, 2009.

[3] A. J. Germond and R. Podmore, "Dynamic aggregation of generating unit models," *IEEE Transactions on Power Apparatus and Systems*, vol. PAS-97, no. 4, pp. 1060–1069, Jul 1978.

[4] J. H. Chow, J. R. Winkelman, M. A. Pai, and P. W. Sauer, "Singular perturbation analysis of large-scale power systems," *International Journal of Electrical Power & Energy Systems*, vol. 12, no. 2, pp. 117–126, Apr 1990.

[5] J. Zaborszky, K.-W. Whang, G. Huang, L.-J. Chiang, and S.-Y. Lin, "A clustered dynamic model for a class of linear autonomous systems unsing simple enumerative sorting," *IEEE Transactions on Circuits and Systems*, vol. 29, no. 11, pp. 747–758, Nov 1982.

[6] J. M. Undrill and A. E. Turner, "Construction of power system electromechanical equivalents by modal analysis," *IEEE Transactions on Power Apparatus and Systems*, vol. PAS-90, pp. 2049–2059, 1971.

[7] I. J. Perez-arriaga, G. C. Verghese, and F. C. Schweppe, "Selective modal analysis with applications to electric power systems, part I: Heuristic introduction," *IEEE Transactions on Power Apparatus and Systems*, vol. PAS-101, no. 9, pp. 3117–3125, Sep 1982.

[8] D. Chaniotis and M. A. Pai, "Model reduction in power systems using Krylov subspace methods," *IEEE Transactions on Power Systems*, vol. 20, no. 2, pp. 888–894, May 2005.

[9] D. Apostolopoulou, P. W. Sauer, and A. D. Domínguez-García, "Balancing authority area model and its application to the design of adaptive AGC systems," *IEEE Transactions on Power Systems*, vol. 31, no. 5, pp. 3756–3764, Sep 2016.

[10] S. S. Guggilam, C. Zhao, E. Dall'Anese, Y. C. Chen, and S. V. Dhople, "Engineering inertial and primary-frequency response for distributed energy resources," in *2017 IEEE 56th Annual Conference on Decision and Control (CDC)*, Dec 2017, pp. 5112–5118.

[11] A. Al-Digs, S. V. Dhople, and Y. C. Chen, "Time-varying injection shift factors to predict post-contingency dynamic line flows," in *Allerton Conference on Communication, Control, and Computing*, Oct 2017, pp. 302–306.

[12] P. W. Sauer and M. A. Pai, *Power System Dynamics and Stability*. Upper Saddle River, NJ: Prentice-Hall, Inc., 1998.

[13] R. A. Horn and C. R. Johnson, *Matrix Analysis*. New York, NY: Cambridge University Press, 2013.

[14] M. D. Ilić and Q. Liu, *Toward Sensing, Communications and Control Architectures for Frequency Regulation in Systems with Highly Variable Resources*. New York, NY: Springer New York, 2012, pp. 3–33.

[15] R. Ramanujam, *Power System Dynamics: Analysis and Simulation*. PHI Learning Pvt. Ltd., 2009.

[16] P. M. Anderson and M. Mirheydar, "A low-order system frequency response model," *IEEE Transactions on Power Systems*, vol. 5, no. 3, pp. 720–729, 1990.

[17] F. Milano, "An open source power system analysis toolbox," *IEEE Trans. on Power Systems*, vol. 20, no. 3, pp. 1199–1206, Aug 2005.